

Fig. 3. Transmission electron micrographs of non-Tg (A, C, E, G) and R75W+ (B, D, F, H) mice. Future space of the tunnel of Corti (asterisk) starts to be formed in non-Tg mice (A), but is not detected in R75W+ mice (B) at P5. At P8, the open space between the IPCs and OPCs below their connection at a tight junction exceeds that of non-Tg mice (arrowhead in C). The TC is insufficient to be created in R75W+ mice (D). At P10, Nuel's space starts to be formed in non-Tg (asterisk in E) but not in R75W+ mice (asterisk in F). At P12, an adult-like configuration of the organ of Corti is created in non-Tg mice (G). The cell cytoplasm of supporting cells is enlarged in R75W+ mice (H). OHCs in R75W+ mice are squeezed by the surrounding DCs (F, H). Scale bar=10 μ m. Abbreviations used: TC, tunnel of Corti; IP, inner pillar cell; OP, outer pillar cell; HC, Hensen cells; CDs, Claudius cells.

remarkable change of the collapse was recognized in the organ of Corti at least from P10 in the light microscopy (data not shown).

Ultrastructural analysis was performed to evaluate the fine structure of the organ of Corti in the late developmental stage. An analysis by TEM demonstrated further details of histological alterations in the organ of Corti (Fig. 3). The opening of tunnel of Corti between the IPC and outer pillar cell (OPC) were seen at P5 in non-Tg mice (Fig. 3A). In contrast, no spaces within IPC and OPC were apparent at P5 onward in R75W+ mice (Fig. 3B). No obvious structural change was observed in the other cells of the organ of Corti at P5. At P8 in both non-Tg and R75W+ mice, during expansion of tunnel of Corti, the pillar cell bodies were distinguished from the surrounding cells (Fig. 3C, 3D). At P10 in non-Tg mice, extensive Nuel's space opening occurred (Fig. 3E). In contrast, the future Nuel's spaces were occupied by bulky processes of Deiter's cells (DCs) in R75W+ mice (Fig. 3F). At P12, non-Tg mice approached a well-matured configuration (Fig. 3G). Supporting cells of R75W+ mice (Fig. 3H) tended to be grossly enlarged as compared with non-Tg. In the R75W+ mice, the IHC from P5 to P12 and the OHC from P5 to P8 had a relatively normal shape. Numerous mitochondria were located along the lateral membrane of the OHCs which was lined by a thick layer of subsurface cisternae (data not shown). However, DCs surrounded and compressed the OHCs at P10–12 (Fig. 3F, 3H).

Both IPCs and OPCs showed a nearly mature appearance, in which abundant microtubules were formed parallel array in non-Tg mice (Fig. 4A) whereas microtubules of the IPCs were poorly formed and hypoplasia occurred in R75W+ mice (Fig. 4B). Actually, the average number of microtubules of the cross-section of the IPCs at P12 in R75W+ mice ($4.4 \pm 3.3/100 \mu\text{m}^2$) was significantly reduced (Fig. 4D) as compared with that of non-Tg mice ($26.9 \pm 25.6/100 \mu\text{m}^2$) (Fig. 4C).

Quantitative data describing peak height and cell areas of the organ of Corti also showed the differences between non-Tg and R75W+ mice (Fig. 5). The height of the organ of Corti in non-Tg mice showed an increase with the development of the organ of Corti as described previously (Souter et al., 1997). In contrast, the height remained unchanged presumably due to collapse of tunnel of Corti in R75W+ mice (Fig. 5A). The cell area of the organ of Corti showed no difference between non-Tg and R75W+ mice at P5, both of which increased rapidly until P8. Although the increase of cell area appeared slowly after the formation of tunnel of Corti and Nuel's space at P8 in non-Tg mice, the area increased from P10 to P12 in R75W+ mice (Fig. 5B). The increase of the cell area from P10–12 recognized in R75W+ mice is assumed to be brought about by the enlarged supporting cells. Thus, the dominant-negative mutant of *Gjb2* disrupted postnatal development of supporting cells.

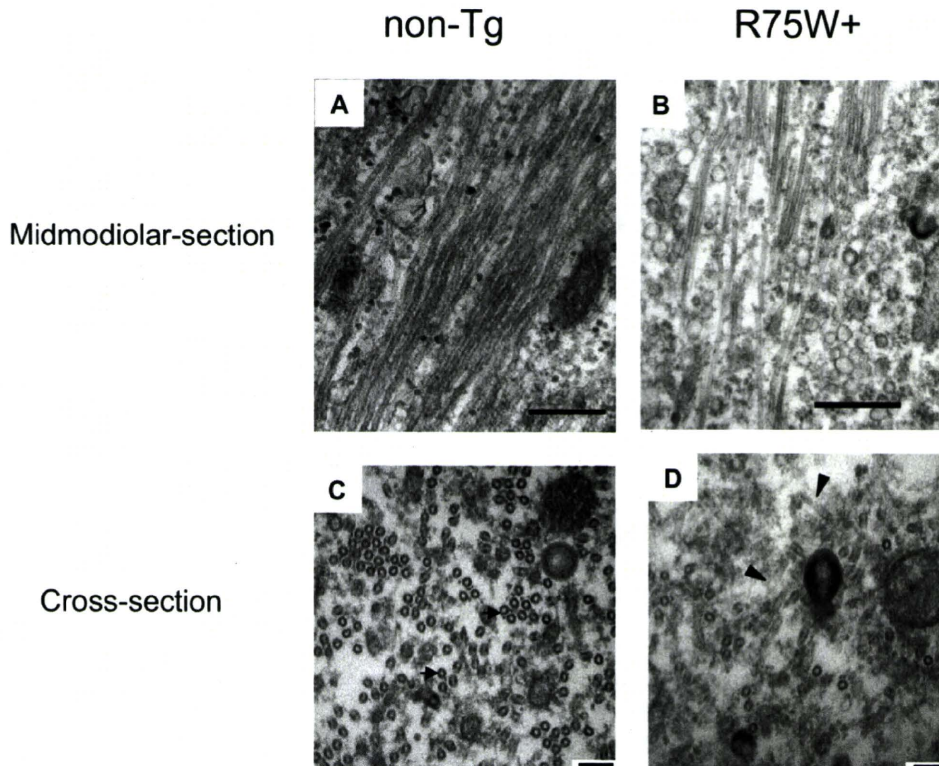


Fig. 4. The microtubules of the midmodiolar- (A, B) and cross-sections (C, D) of the IPC at P12. The microtubules are rich in the IPC in non-Tg mice (arrows in A). The microtubules of the IPC are poorly formed and hypoplasia in R75W+ mice (arrows in B). Round-shaped microtubules with cross-sections are abundant in non-Tg mice (arrows in C). (D) The number of microtubules is reduced and the tangled microtubules (arrows in D) are prominent in R75W+ mice. Scale bar=500 nm (A, B); 1 μm (C, D).

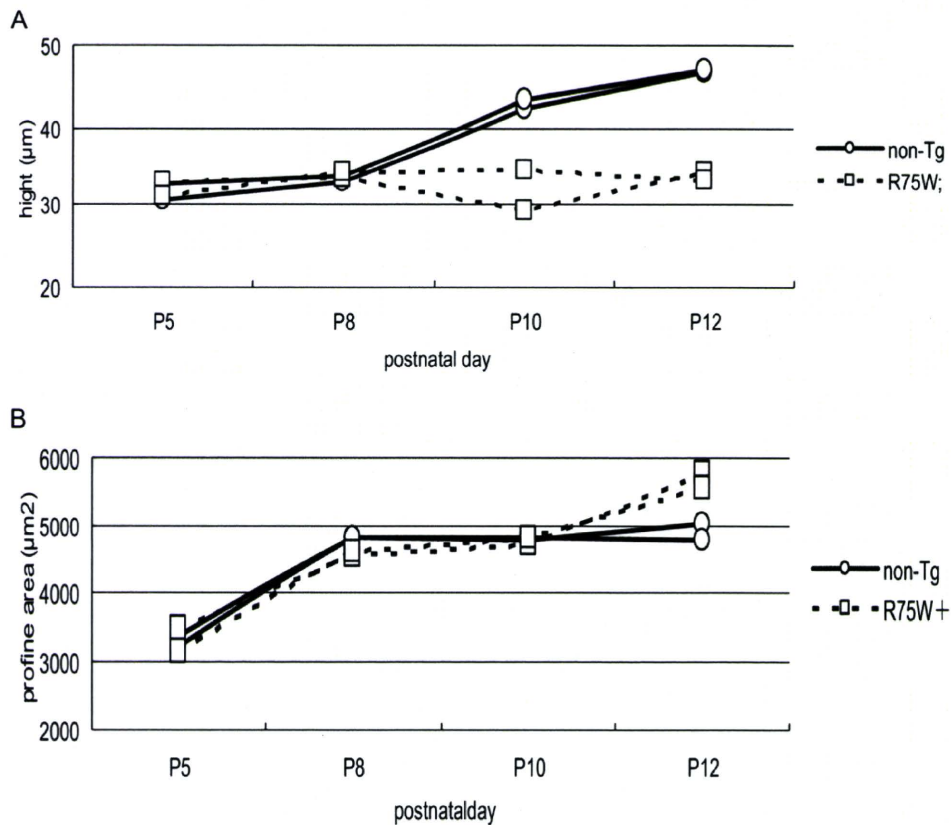


Fig. 5. The height of (A) and cell area (B) of the organ of Corti in individual mice of non-Tg ($n=2$) and R75W+ ($n=2$). R75W+ mice show the reduction of the height of the organ of Corti from P10 as compared with non-Tg mice (A). At P12, the profile area of the organ of Corti of R75W+ mice is greater than that of non-Tg mice (B).

Since it is possible that the *Gjb2* gene affects the known genes to determine or differentiate regarding hair or supporting cells, the protein expression of FGFR3 and p27^{Kip1} for supporting cell markers, and MyosinVIIa for a hair cell marker were examined at P12. Similar results regarding the immunolabeling of the cochlear section for the tested antibodies were obtained in both R75W+ and non-Tg mice (Fig. 6).

DISCUSSION

The present study demonstrated that ABR have never been recognized in the postnatal stage of R75W+ mice from P5 to P14. On the other hand, non-Tg mice showed the onset of ABR at P11, which approached near maturity until P14. These findings may be explained by the supposition that the cochlear function does not reach maturation in a dominant-negative mutation of *Gjb2*.

The characteristic changes of ultrastructures observed in the developing non-sensory cells of the organ of Corti include: i) absence of tunnel of Corti, Nuel's space, or spaces surrounding the OHCs; ii) significant small numbers of microtubules in IPCs; iii) shortening of height of the organ of Corti; and iv) increase of the midmodiolar-sectional area of the cells of the organ of Corti. Thus, morphological observations confirmed that a dominant-negative *Gjb2* mutation showed incomplete development of the

cochlear supporting cells. On the other hand, the development of the sensory hair cells at least from P5 to P12 was not affected, which is not surprising since the sensory hair cells do not express Cx26 throughout development. In fact, *MyosinVIIa*, a major gene identified in hair cells was expressed in the developing hair cells of R75W+ mice.

Our dominant-negative *Gjb2* mutant mice showed a phenotype apparently different from that of a target disruption of *Gjb2* (Cohen-Salmon et al., 2002), in which the inner ear normally developed up to P14 followed by the degeneration of the cochlear epithelial networks and sensory hair cells. Furthermore, our preliminary study (Ikeda et al., 2004) in a creation of a conditional knockout of *Gjb2* using the promoter different from that of Cohen-Salmon et al. (2002) showed comparable findings to the present dominant-negative *Gjb2* mutant. Both animal models of *Gjb2*-based hereditary deafness developed by us strongly indicate that *Gjb2* is indispensable throughout the postnatal development of the organ of Corti, especially from P5 to maturation.

The development of pillar cells and the formation of a normal tunnel of Corti are required for normal hearing (Colvin et al., 1996). The factors that regulate pillar cells development are *Fgfr3* (Mueller et al., 2002). The mice homozygous for a targeted disruption of *Fgfr3* had striking inner ear defects and were deaf. In the organ of Corti of

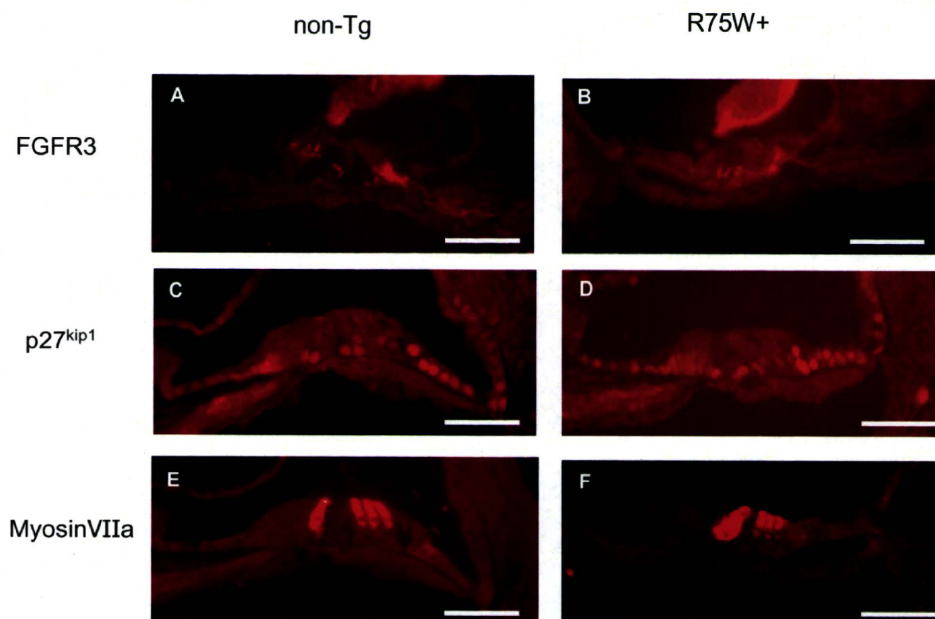


Fig. 6. Immunohistochemical analysis of the inner ear. Expressions of the FGFR3 are specifically localized in pillar cells in both non-Tg (A) and R75W+ (B). Expressions of the p27^{Kip1} are labeled in nucleus of supporting cells in both non-Tg (C) and R75W+ (D). The inner and OHCs are labeled with MyosinVIIa in both non-Tg (E) and R75W+ (F). Scale bar=100 μ m.

Fgfr3 deficient mice, differentiated pillar cells and the tunnel space were completely absent and ABR showed no response at 100 dB SPL (Colvin et al., 1996), which is interesting as it is similar to the observations of our R75W+ mice. It is possible that the cochlear *Gjb2* regulates differentiation genes of the supporting cells at the transcriptional or translational level. However, the expression of *Fgfr3* and p27^{Kip1} proteins in the R75W+ mouse cochlea was equivalent to those of non-Tg mouse, which seems to negate the involvement of *Fgfr3* and p27^{Kip1} genes to the disrupted differentiation of pillar cells and other supporting cells. It is possible to cause the effect similar to *Fgfr3* disruption by mediating its upstream and downstream pathways. Further studies are required to obtain a better understanding of the relevance of the *Fgfr3* pathway. The mutant mice of thyroid hormonal receptors were reported to have delayed postnatal development of the organ of Corti (Rusch et al., 2001). The phenotype of thyroid hormonal receptor mutants is similar to our phenotype with respect to the unopened tunnel of Corti, but not to the formation of tectorial membrane or the development of EP. Although the typical distribution of prestin along the OHC lateral membrane was found to depend on the thyroid hormone receptor TR β (Winter et al., 2006), prestin was normally expressed in our Tg mice (our unpublished observations). These findings suggest that thyroid hormone is not related to the phenotype of the *Gjb2* dominant-negative mutation.

The results presented here demonstrate a significant reduction of the number of microtubules in the pillar cells in R75W+ mice, which presumably causes absence of the tunnel and incomplete height of the organ of Corti. The microtubules in the pillar cells appear to be unique to mammalian cochlea with respect to the aspect of a strong

and rigid cytoskeleton for maintenance of cell shape and effective transduction of vibratory stimuli on the sensory epithelium (Saito and Hama, 1982; Slepecky et al., 1995). The disturbed formation of microtubules in DCs, which were not evaluated in the present study, is expected to take a place similar to pillar cells and may lead to failure to form Nuel's space as well as a lack of DC cup surrounding the hair cells and the nerve ending.

Morphometric analysis of cross-sectional areas of the cells of the organ of Corti suggests the reduction of cell volume whereas extracellular spaces such as tunnel of Corti, Nuel's space, and spaces surrounding OHCs were apparently diminished under the TEM observation. Inhibitory effects of channels, transporters, and fluid secretion are suspected to be mediated by cell-signal molecules through the gap junctions (Beltramello et al., 2005; Lang et al., 2007; Piazza et al., 2007; Zhang et al., 2005; Zhao et al., 2005). K-Cl cotransporters encoded by *Kcc3* and *Kcc4* are selectively expressed in DCs from late postnatal development and are thought to regulate the cell volume and the ionic environment of cortilymph (Boettger et al., 2002, 2003). The mouse cochlea deleting *Kcc3* or *Kcc4* resemble the phenotype of our R75W+ mice, implying that the increase of sectional-area of the cells of the organ of Corti may involve dysfunction of K-Cl cotransport in the DCs of R75W+ mice. The progressive degeneration of hair cells observed in the adult R75W+ mice (Kudo et al., 2003) may be brought about by the changes in the ionic composition of the cortilymph surrounding the basolateral surface of the hair cells (Ben-Yosef et al., 2003).

Gap junction proteins in the cochlear supporting cells are hypothesized to allow rapid removal of K⁺ away from the base of hair cells, resulting in recycling back to the endolymph (Kikuchi et al., 1995). In addition to the K⁺

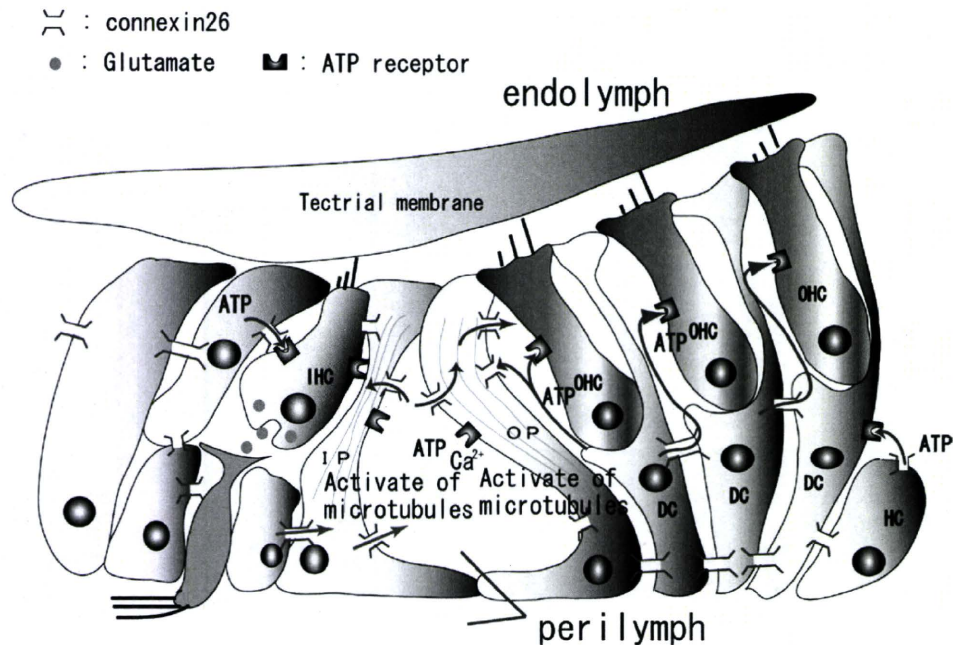


Fig. 7. Hypothesized schematic diagram of proposed intercellular signaling pathways between supporting cells and hair cells in the cochlea. ATP released from supporting cells via connexin hemichannels activates purinergic receptors on the hair cells or supporting cells in an autocrine and paracrine manner. Defective Cx26 is postulated to disrupt depolarization in the IHC and OHC, which may influence the glutamate release and the production of neurotrophic factors, respectively. Moreover, the failure of polymerization of the microtubules in the pillar cells may result from the disturbance of ATP release and/or intercellular signal transduction.

recycling theory, Ca^{2+} and anions such as inositol 1,4,5-trisphosphate, ATP, and cAMP are mediated by gap junction proteins to act as cell-signaling and nutrient and energy molecules (Beltramello et al., 2005; Piazza et al., 2007; Zhang et al., 2005; Zhao et al., 2005). More currently, Tritsch et al. (2007) found that, in the postnatal immature cochlea, a transient structure known as Kölliker organ releases ATP through the hemichannels of its gap junctions, which binds to P2X receptors on the IHCs to cause depolarization and Ca^{2+} influx, mimicking the effect of sound. The resulting release of glutamate activates receptors on the afferent fibers, which is essential for the development of the auditory pathway. ATP is known to act as trophic factor, mitogen and potent neuromodulator (Fields and Burnstock, 2006; Nedergaard et al., 2003). Since supporting cells express ATP receptors (Dulon et al., 1993), the same scenario is likely to occur in an adapted form with the organ of Corti. The supporting cells may have an influence on maturation, cell volume and cell shape at least through the polymerization of microtubules by activated by ATP in an autocrine and paracrine manner (Zhao et al., 2005). We propose the hypothesis of an underlying mechanism to explain the prelingual deafness caused by *Gjb2* mutation (Fig. 7). Defective gap junction impairs the release of ATP and other factors related to cell-signaling and nutrient and energy molecules, resulting in the disturbance of normal postnatal development of the organ of Corti. Postnatal maturation of the various cochlear cells in the organ of Corti rapidly and synchronously progressed at P5 to P12 and may be regulated by intercellular signal transduction mediated by ions and biomodulators via the

gap junction network derived from Cx26. Furthermore, a similar hypothesis may involve the postnatal development of the stria vascularis and spiral ligament because of the presence of purinergic receptors (Ikeda et al., 1995; Liu et al., 1995; Ogawa and Schacht, 1995) and the source of ATP (White et al., 1995; Suzuki et al., 1997).

CONCLUSION

In conclusion, the present findings strongly support that *Gjb2* is indispensable in the postnatal development of the organ of Corti and normal hearing.

Acknowledgments—This work was supported in part by research grant from the Ministry of Education, Science, and Culture of Japan (Nos. 16209050, 17659538, and 19659441) and Uehara Memorial Foundation.

REFERENCES

- Anniko M (1983) Postnatal maturation of cochlear sensory hairs in the mouse. *Anat Embryol (Berl)* 166:355–368.
- Beltramello M, Piazza V, Bukauskas FF, Pozzan T, Mammano F (2005) Impaired permeability to Ins(1,4,5)P₃ in a mutant connexin underlies recessive hereditary deafness. *Nat Cell Biol* 2005 7:63–69.
- Ben-Yosef T, Belyantseva IA, Saunders TL, Hughes ED, Kawamoto K, Van Itallie CM, Beyer LA, Halsey K, Gardner DJ, Wilcox ER, Rasmussen J, Anderson JM, Dolan DF, Forge A, Raphael Y, Camper SA, Friedman TB (2003) Claudin 14 knockout mice, a model for autosomal recessive deafness DFNB29, are deaf due to cochlear hair cell degeneration. *Hum Mol Genet* 12:2049–2061.

- Boettger T, Hübner CA, Maier H, Rust MB, Beck FX, Jentsch TJ (2002) Deafness and renal tubular acidosis in mice lacking the K-Cl co-transporter *Kcc4*. *Nature* 416:874–878.
- Boettger T, Rust MB, Maier H, Seidenbecher T, Schweizer M, Keating DJ, Faulhaber J, Ehrhke H, Pfeffer C, Scheel O, Lemcke B, Horst J, Leuwer R, Pape HC, Völkl H, Hübner CA, Jentsch TJ (2003) Loss of K-Cl co-transporter *KCC3* causes deafness, neurodegeneration and reduced seizure threshold. *EMBO J* 22:5422–5434.
- Cohen-Salmon M, Ott T, Michel V, Hardelin JP, Perfettini I, Eybalin M, Wu T, Marcus DC, Wangemann P, Willecke K, Petit C (2002) Targeted ablation of connexin26 in the inner ear epithelial gap junction network causes hearing impairment and cell death. *Curr Biol* 12:1106–1111.
- Colvin JS, Bohne BA, Harding GW, McEwen DG, Ornitz DM (1996) Skeletal overgrowth and deafness in mice lacking fibroblast growth factor receptor 3. *Nat Genet* 12:390–397.
- Dulon D, Moataz R, Mollard P (1993) Characterization of Ca^{2+} signals generated by extracellular nucleotides in supporting cells of the organ of Corti. *Cell Calcium* 14:245–254.
- Elias LA, Wang DD, Kriegstein AR (2007) Gap junction adhesion is necessary for radial migration in the neocortex. *Nature* 448:901–907.
- Faddis BT, Hughes RM, Miller JD (1998) Quantitative measures reflect degeneration, but not regeneration, in the deafness mouse organ of Corti. *Hear Res* 115:6–12.
- Fields RD, Burnstock G (2006) Purinergic signaling in neuron-glia interactions. *Nat Rev Neurosci* 7:423–436.
- Frenz CM, Van de Water TR (2000) Immunolocalization of connexin 26 in the developing mouse cochlea. *Brain Res Rev* 32:172–180.
- Gabriel HD, Jung D, Butzler C, Temme A, Traub O, Winterhager E, Willecke K (1998) Transplacental uptake of glucose is decreased in embryonic lethal connexin26-deficient mice. *J Cell Biol* 140:1453–1461.
- Ikeda K, Kudo T, Jin ZH, Gotoh S, Katori Y, Kikuchi T, Minowa O, Noda T (2004) Conditional gene targeting of *Gjb2* results in profound deafness due to maturation failure of the organ of Corti. 27th Midwinter research meeting, #762.
- Ikeda K, Suzuki M, Furukawa M, Takasaka T (1995) Calcium mobilization and entry induced by extracellular ATP in the non-sensory epithelial cell of the cochlear lateral wall. *Cell Calcium* 18:89–99.
- Kikuchi T, Kimura RS, Paul DL, Adams JC (1995) Gap junctions in the rat cochlea: immunohistochemical and ultrastructural analysis. *Anat Embryol* 191:101–118.
- Kudo T, Kure S, Ikeda K, Xia AP, Katori Y, Suzuki M, Kojima K, Ichinohe A, Suzuki Y, Aoki Y, Kobayashi T, Matsubara Y (2003) Transgenic expression of a dominant-negative connexin26 causes degeneration of the organ of Corti and non-syndromic deafness. *Hum Mol Genet* 12:995–1004.
- Lang F, Vallon V, Knipper M, Wangemann P (2007) Functional significance of channels and transporters expressed in the inner ear and kidney. *Am J Physiol Cell Physiol* 293:C1187–C1208.
- Liu J, Kozakura K, Marcus DC (1995) Evidence for purinergic receptors in vestibular dark cell and stria marginal cell epithelia of the gerbil. *Auditory Neurosci* 1:331–340.
- Mueller KL, Jacques BE, Kelly MW (2002) Fibroblast growth factor signaling regulates pillar cell development in the organ of Corti. *J Neurosci* 22:9368–9377.
- Nedergaard M, Ransom B, Goldman SA (2003) New roles for astrocytes: redefining the functional architecture of the brain. *Trends Neurosci* 26:523–530.
- Ogawa K, Schacht J (1995) P2y purinergic receptors coupled to phosphoinositide hydrolysis in tissues of the cochlear lateral wall. *Neuroreport* 6:1538–1540.
- Piazza V, Ciubotaru CD, Gale JE, Mammano F (2007) Purinergic signalling and intercellular Ca^{2+} wave propagation in the organ of Corti. *Cell Calcium* 41:77–86.
- Rusch A, Ng L, Goodyear R, Oliver D, Lisoukov I, Vennstrom B, Richardson G, Kelley MW, Forrest D (2001) Retardation of cochlear maturation and impaired hair cell function caused by deletion of all known thyroid hormone receptors. *J Neurosci* 21:9792–9800.
- Saito K, Hama K (1982) Structural diversity of microtubules in the supporting cells of the sensory epithelium of guinea pig organ of Corti. *J Electron Microsc* 31:278–281.
- Slepecky NB, Henderson CG, Saha C (1995) Post-translational modifications of tubulin suggest that dynamic microtubules are present in sensory cells and stable microtubules are present in supporting cells of the mammalian cochlea. *Hear Res* 91:136–147.
- Souter M, Nevill G, Forge A (1997) Postnatal maturation of the organ of Corti in gerbils: morphology and physiological responses. *J Comp Neurol* 386:635–651.
- Suzuki H, Ikeda K, Furukawa M, Takasaka T (1997) P2 purinoceptor of the globular substance in the otoconial membrane of the guinea pig inner ear. *Am J Physiol* 273:C1533–C1540.
- Tritsch NX, Yi E, Gale JE, Glowatzki E, Bergles DE (2007) The origin of spontaneous activity in the developing auditory system. *Nature* 450:50–55.
- White PN, Thorne PR, Housley GD, Mockett B, Billett TE, Burnstock G (1995) Quinacrine staining of marginal cells in the stria vascularis of the guinea-pig cochlea: a possible source of extracellular ATP? *Hear Res* 90:97–105.
- Winter H, Braig C, Zimmermann U, Geisler HS, Fränzer JT, Weber T, Ley M, Engel J, Knirsch M, Bauer K, Christ S, Walsh EJ, McGee J, Köpfschall I, Rohbock K, Knipper M (2006) Thyroid hormone receptors TRalpha1 and TRbeta differentially regulate gene expression of *Kcnq4* and *prestin* during final differentiation of outer hair cells. *J Cell Sci* 119:2975–2984.
- Zhang Y, Tang W, Ahmad S, Sipp JA, Chen P, Lin X (2005) Gap junction-mediated intercellular biochemical coupling in cochlear supporting cells is required for normal cochlear function. *Proc Natl Acad Sci U S A* 102:15201–15206.
- Zhao HB, Yu N, Fleming CR (2005) Gap junctional hemichannel-mediated ATP release and hearing controls in the inner ear. *Proc Natl Acad Sci U S A* 102:18724–18729.

(Accepted 11 August 2008)
(Available online 22 August 2008)

Brief Report

Noninvasive *In Vivo* Delivery of Transgene via Adeno-Associated Virus into Supporting Cells of the Neonatal Mouse Cochlea

TAKASHI IIZUKA,¹ SHO KANZAKI,² HIDEKI MOCHIZUKI,³ AYAKO INOSHITA,¹ YUYA NARUI,¹ MASAYUKI FURUKAWA,¹ TAKESHI KUSUNOKI,¹ MAKOTO SAJI,⁴ KAORU OGAWA,² and KATSUHISA IKEDA¹

ABSTRACT

There are a number of genetic diseases that affect the cochlea early in life, which require normal gene transfer in the early developmental stage to prevent deafness. The delivery of adenovirus (AdV) and adeno-associated virus (AAV) was investigated to elucidate the efficiency and cellular specificity of transgene expression in the neonatal mouse cochlea. The extent of AdV transfection is comparable to that obtained with adult mice. AAV-directed gene transfer after injection into the scala media through a cochleostomy showed transgene expression in the supporting cells, inner hair cells (IHCs), and lateral wall with resulting hearing loss. On the other hand, gene expression was observed in Deiters cells, IHCs, and lateral wall without hearing loss after the application of AAV into the scala tympani through the round window. These findings indicate that injection of AAV into the scala tympani of the neonatal mouse cochlea therefore has the potential to efficiently and noninvasively introduce transgenes to the cochlear supporting cells, and this modality is thus considered to be a promising strategy to prevent hereditary prelingual deafness.

INTRODUCTION

SEVERAL TYPES OF HEREDITARY DEAFNESS in humans have been matched with homologous mouse models (Eisen and Ryugo, 2007). Mice present an ideal model for inner ear gene therapy because their genome is being rapidly sequenced and their generation time is relatively short. To achieve effective gene therapy in hereditary deafness, it may be required to transfer corrective genes into the defective cochlear cells of neonatal mice. However, the small size of the neonatal mouse inner ear poses a particular challenge for performing surgical procedures.

Transgene expression has been successfully demonstrated in the mammalian inner ear, using various viral vectors including adenoviral (AdV) vectors (Raphael *et al.*, 1996), adeno-associated viral (AAV) vectors (Lalwani *et al.*, 1996), herpes simplex

viral vectors (Derby *et al.*, 1999), lentiviral vectors (Han *et al.*, 1999), and Sendai viral vectors (Kanzaki *et al.*, 2007). In this study, we tested AAV vectors and AdV vectors because AAVs are free of genotoxicity and present no evidence of pathogenicity in humans, and AdVs have high transfection efficiency in many tissues and cell types. In previous studies, the three main routes of delivery of viral vectors into the cochlea of the adult mouse, namely, the scala media approach, the semicircular canal approach, and the round window (RW) approach, have been reported (Kawamoto *et al.*, 2001; Suzuki *et al.*, 2003). The semicircular canal method was not used in this study because of its poor transduction of genes.

The present study assessed how to inject a gene into the neonatal mouse cochlea on postnatal day 0 (P0); the results indicate that this modality is a promising therapeutic strategy to prevent prelingual deafness.

¹Department of Otorhinolaryngology, Juntendo University School of Medicine, Tokyo 113-8421, Japan.

²Department of Otolaryngology, Keio University, Tokyo 160-0016, Japan.

³Department of Neurology, Juntendo University School of Medicine, Tokyo 113-8421, Japan.

⁴Department of Physiology, School of Allied Health Sciences, Kitasato University, Sagami-hara 228-8555, Japan.

MATERIALS AND METHODS

Animals

Twenty healthy C57BL/6 mouse pups, irrespective of gender, were used on P0 (within 24 hr of birth). All experimental protocols were approved by the Institutional Animal Care and Use Committee at Juntendo University (Tokyo, Japan), and were conducted in accordance with the U.S. National Institutes of Health *Guide for the Care and Use of Laboratory Animals*.

Adenoviral and adeno-associated viral vectors

A replication-deficient adenoviral vector (human AdV, serotype 5) was used to encode the green fluorescent protein (GFP) driven by the cytomegalovirus (CMV) promoter. The virus was designated Ad5.CMV-GFP (3×10^{11} plaque-forming units [PFU]/ml). The E1 and E3 regions were deleted. Vectors were purchased from Primmune KK (Osaka, Japan). Viral suspensions in 10 mM Tris-HCl (pH 7.5), 1 mM MgCl₂, and 10% glycerol were kept at -80°C until thawed for use.

The plasmid DNA pAAV-MCS (CMV promoter; Stratagene, La Jolla, CA) carrying the GFP gene was constructed as reported previously (Yamada *et al.*, 2004). The plasmid DNA pAAV-GFP was cotransfected with plasmids pHelper and Pack2/1 into HEK-293 cells, using the standard calcium phosphate method (Sambrook and Russell, 2001). After 48 hr, cells were harvested and crude recombinant AAV (rAAV) vector (serotype 1) solutions were obtained by repeated freeze-thaw cycles. After ammonium sulfate precipitation, the viral particles were dissolved in phosphate-buffered saline (PBS) and applied to an OptiSeal centrifugation tube (Beckman Coulter, Fullerton, CA). After overlaying OptiPrep solution (Axis-Shield PoC, Oslo, Norway), the tube was processed with a Gradient Master (BioComp Instruments, Fredericton, NB, Canada) to prepare a gradient layer of OptiPrep. The tube was then ultracentrifuged at 13,000 rpm for 18.5 hr. The fractions con-

taining high-titer rAAV vectors were collected and used for injection into animals. The number of rAAV genome copies was semiquantified by polymerase chain reaction (PCR) within the CMV promoter region using primers 5'-GACGTCAATAATGACGTATG-3' and 5'-GGTAATAGCGATGACTAATACG-3'. The final titer was 1.4×10^{13} viral particles (VP)/ml.

Surgical procedures

Glass capillaries (Drummond Scientific, Broomall, PA) were drawn with a PB-7 pipette puller (Narishige, Tokyo, Japan) to achieve an approximately 10- μm outer tip diameter. A polyethylene tube (outer diameter, 1.7 mm; Atom Medical, Saitama, Japan) was connected to the glass micropipette.

For injection into the scala media via a cochleostomy, C57BL/6 mice were anesthetized with ketamine (100 mg/kg) and xylazine (4 mg/kg) by intraperitoneal injection. A left postauricular incision was made and the otic bulla was exposed, and opened to expose the cochlea. A cochleostomy was made at the cochlear lateral wall of a basal turn just beneath the stapedia artery with the glass micropipette, using a micromanipulator. The bony lateral wall of the cochlea on P0 is so soft that it can be easily penetrated by the glass micropipette. The injection volume of the viral vector was regulated at approximately 0.02 $\mu\text{l}/\text{min}$ for 10 min, using a syringe connected to the polyethylene tube. To allow the vector to spread throughout and stabilize in the inner ear, the glass micropipette was left in place for 1 min after the injection. The hole was plugged and the opening in the tympanic bulla was sealed with connective tissue. The total surgical period was approximately 20 min.

For injection into the scala tympani after anesthesia, the otic bulla was opened to expose the RW. Next, the glass micropipette was inserted into the RW (Fig. 1), and the vectors were injected in the same manner as in the scala media approach. Because the hole in the RW membrane was extremely small, leakage of perilymph was found to be nominal after re-

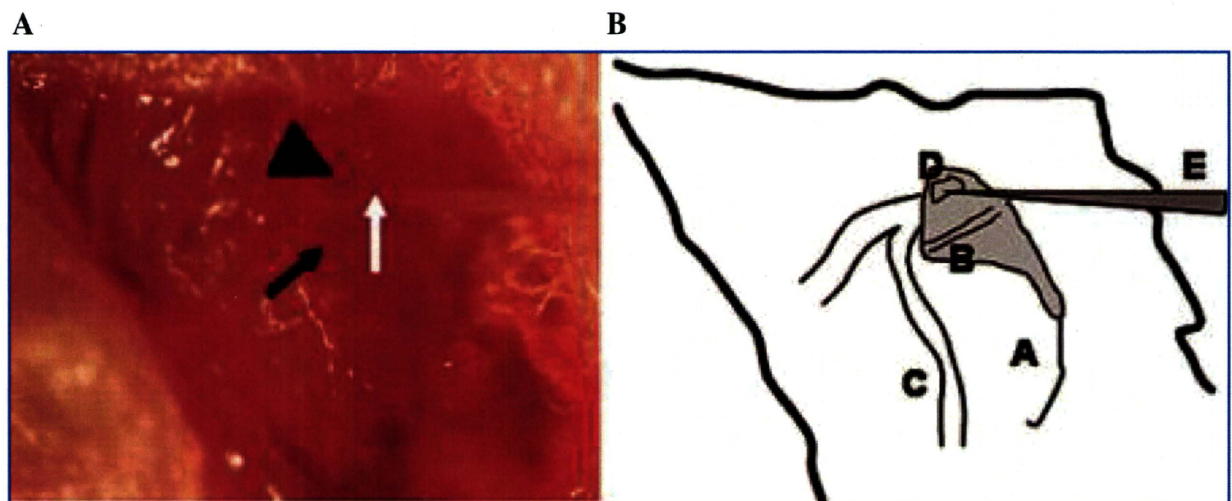


FIG. 1. Surgical procedure for microinjection into the neonatal mouse cochlea. The otic bulla was exposed after a left postauricular incision. The otic bulla is transparent. After opening the otic bulla, a round window (arrowhead) and the stapedia artery (solid arrow) are seen. Viral vectors were injected into the scala tympani with a glass micropipette (open arrow) inserted into the RW membrane. A, tympanic bulla; B, stapedia artery; C, facial nerve; D, round window; E, glass micropipette.

moving the micropipette. It took approximately 20 min to complete the surgical procedure. After the surgery, the mice were kept in another cage until they awoke from anesthesia.

Measurements of auditory brainstem response

To determine the surgical effects on auditory function, the auditory brainstem response (ABR) were assessed 14 days post-operatively. Hearing thresholds were determined in both ears: the injected side (left) and the contralateral noninjected control side (right). ABR measurements were performed as previously reported (Kanzaki *et al.*, 2007). Thresholds were determined for frequencies of 4, 8, 12, 16, and 20 kHz from a set of responses at various intensities with 5-dB intervals and electrical signals were averaged at 512 repetitions. If the hearing threshold was over 95 dB, then it was determined to be 100 dB.

Sample preparation, histology, and immunohistochemical analysis

On day 14 after injection, the mice were deeply anesthetized and perfused intracardially with PBS, followed by 4% paraformaldehyde in phosphate buffer. The cochleae were excised and then tissue specimens were fixed in 4% paraformaldehyde for 2 hr and decalcified in 0.12 M EDTA for 7 days at room temperature. For frozen sections, specimens were cryoprotected in 30% sucrose in PBS overnight at 4°C, and then were embedded, frozen, and sectioned at 10 μ m. For immunofluorescence, sections were incubated with 50% Block Ace (AbD Serotec/MorphoSys, Martinsried, Germany) in PBS–0.3% Triton X-100 for 60 min and then they were incubated overnight at 4°C with goat polyclonal anti-GFP antibodies (diluted 1:200 in PBS; Santa Cruz Biotechnology, Santa Cruz, CA). The next day, tissue specimens were rinsed with PBS, incubated for 60 min with rabbit anti-goat IgG antibodies conjugated with Alexa Fluor 488 (diluted 1:500; Invitrogen Molecular Probes, Eugene, OR), and rinsed with PBS. Subsequently, all specimens were incubated with rhodamine phalloidin (diluted 1:100; Invitrogen Molecular Probes) for 30 min and then were mounted in VECTASHIELD antifade mounting medium with 4',6-diamidino-2-phenylindole (DAPI; Vector Laboratories, Burlingame, CA).

Images of sections were captured with a Zeiss Axioplan 2 microscope (Carl Zeiss, Oberkochen, Germany), using an AxioCam HRc charge-coupled device (CCD) camera and the AxioVision release 4.5 software program.

Data analysis

The KaleidaGraph statistical software program (Synergy Software, Reading, PA) was used for the statistical analysis of the ABR data.

RESULTS

All of the animals recovered uneventfully from surgery and survived until ABR measurements were performed. No signs of vestibular disturbance, such as circling behavior or head tilting, were observed.

After the injection of AdV vectors into the scala media ($n = 3$), GFP-positive cells were present mainly in the supporting cells (Fig. 2A), mesothelial cells of the scala tympani and scala vestibuli, and cells of Reissner's membrane. Injection of AdV through the RW ($n = 5$) induced the expression of GFP only in the mesothelial cells lining the perilymphatic spaces (Fig. 2B). No GFP-positive cells were found in either the organ of Corti or the lateral wall. GFP expression was identified in various cochlear cells (Fig. 2C), predominantly in both the inner hair cells and the supporting cells of the organ of Corti after AAV injection into the scala media ($n = 6$), and the loss of hair cells, as noted in a previous report (Ishimoto *et al.*, 2002), was not observed in these mice (Fig. 2D). Application of AAV to the scala tympani across the RW ($n = 6$) showed that GFP-positive cells were found mainly in the supporting cells (Fig. 2E), and loss of hair cells was not (Fig. 2F). These results are summarized in Table 1. An examination of the contralateral (right) ears of AAV injected mice revealed a normal appearance with no pathological hair cell loss, and no GFP-positive cells were seen (Fig. 2G and H).

Before killing the mice on P14, ABR thresholds were assessed in both ears, on both the injected side and contralateral side. In the groups injected with AAV (Fig. 3A) or AdV vectors (Fig. 3B) by the scala tympani approach through the RW, the ABR thresholds did not differ significantly from those of contralateral noninjected control sides at any frequency tested. On the other hand, a significant threshold shift at each frequency was seen in the group injected with either AAV (Fig. 3C) or AdV vectors (Fig. 3D) by the scala media approach via cochleostomy, in comparison with those on the contralateral control sides.

DISCUSSION

To our knowledge this is the first report demonstrating successful gene delivery to the neonatal mouse cochlea *in vivo*. It is ideal to transfer a normal gene noninvasively to a hereditary deafness mouse model at an early time after birth, before differentiation of the cochlear sensory structures. The procedure of gene delivery to the animal models must yield efficient gene transduction without hearing loss.

Excellent gene expression without hearing loss was obtained by selecting both the appropriate application route (the

FIG. 2. Sagittal cryosections of the mouse cochlea. GFP-expressing cells (green) are seen by fluorescence microscopy in cochlear sagittal cryosections of P14 mice that had been injected on P0. Rhodamine phalloidin antibody was used as a marker for hair cells (red). (A) Cochlear section after exposure to AdV by scala media injection. Transduced Deiters cells and outer pillar cells (arrows) expressed GFP. (B) After exposure to AdV by scala tympani injection. Only mesothelial cells of the perilymph expressed GFP. GFP were absent in the organ of Corti. (C and D) Cochlear section after exposure to AAV by scala media injection. (C) Transduced supporting cells (Deiters cells, Hensen cells, and Claudius cells; arrowheads) expressed GFP. (D) No loss of hair cells was observed with the nuclear label DAPI (blue). (E and F) After exposure to AAV by scala tympani injection, transduced Deiters cells (arrows) expressed GFP (E), and loss of hair cells was not observed (F). (G and H) Cochlear section of contralateral (right) ears after exposure to AAV by both scala media injection (G) and scala tympani injection (H) revealed a normal appearance with no pathological hair cell loss, and no GFP-positive cells were seen. Scale bar in (A) (for A–H): 100 μ m.

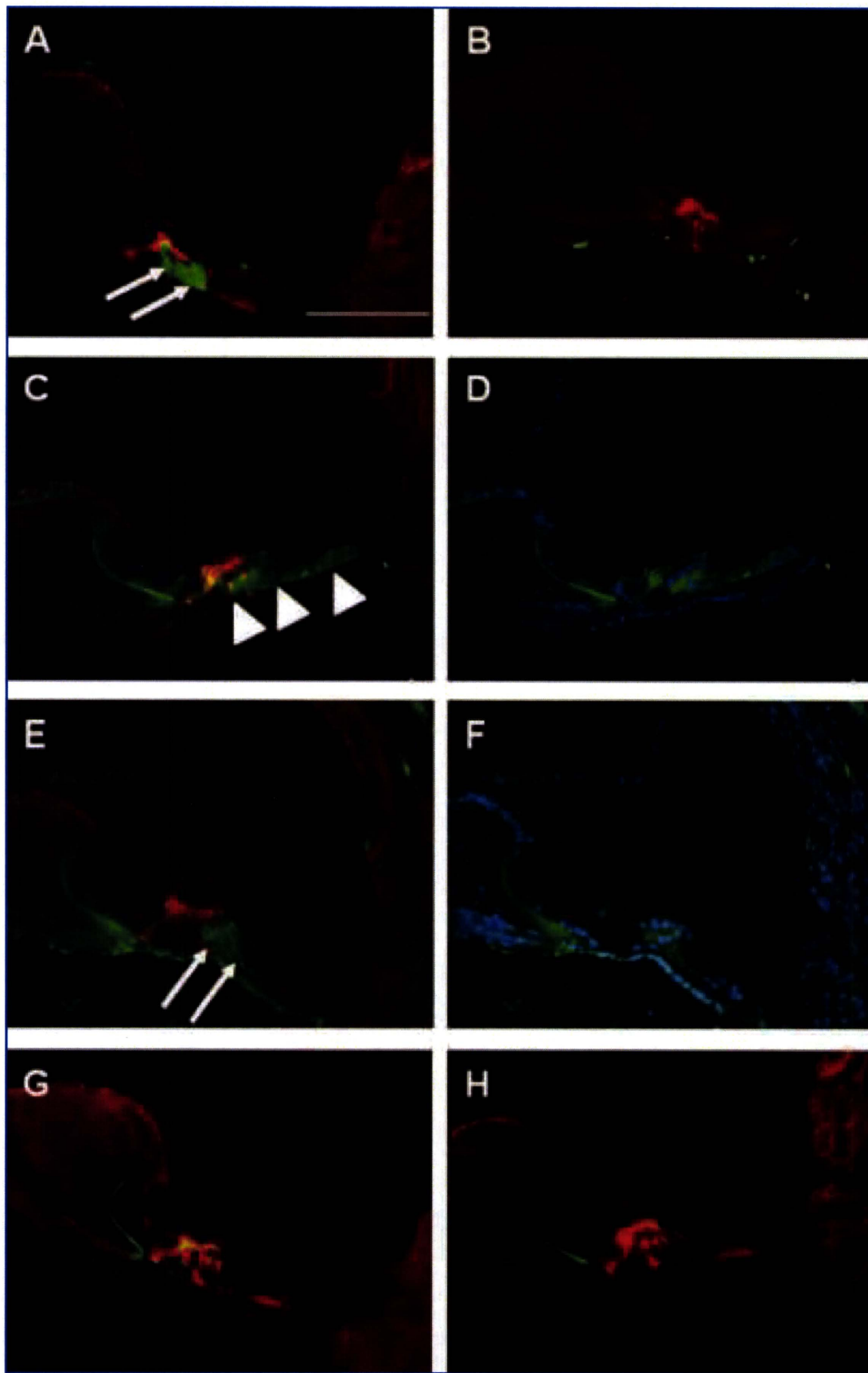


FIG. 2.

TABLE 1. EXPRESSION OF TRANSGENE IN MOUSE COCHLEAR CELLS

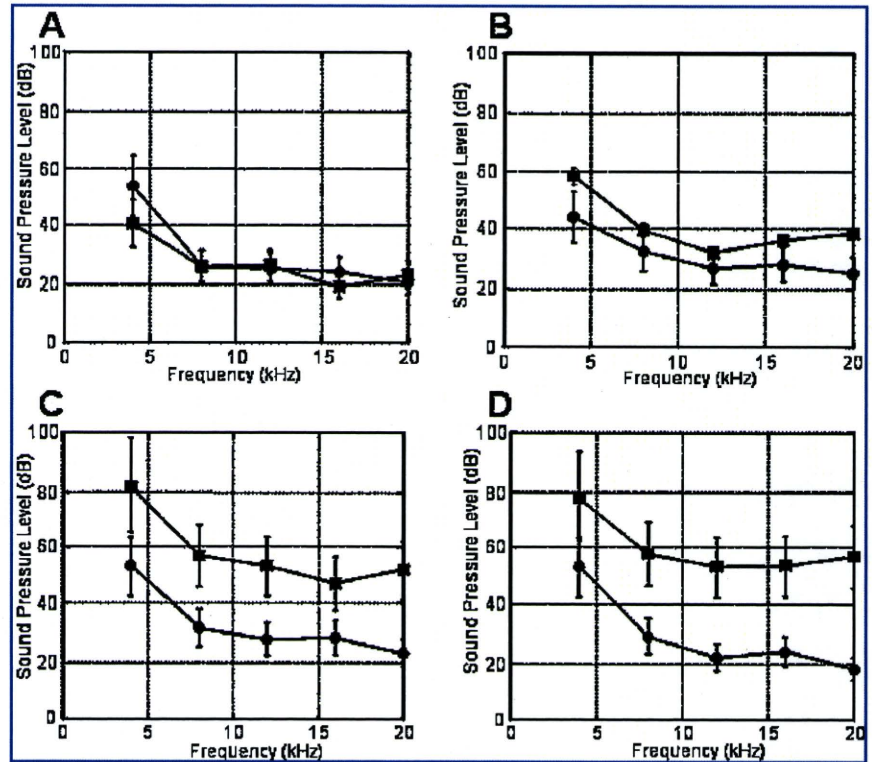
Vector	Injection place	Total number	Inner hair cells	Outer hair cells	Pillar cells	Deiters cells	Hensen cells	Claudious cells	Inner sulcus cells	Outer sulcus cells	Stria vascularis	Spiral ganglion	Spiral ligament	Reissner's membrane	Spiral limbus	Mesothelial cells
AAV	RW	n = 6	6	—	—	5	4	3	2	2	4	2	6	1	2	5
	Cochleostomy	n = 6	6	1	1	5	5	5	4	5	5	—	6	3	6	5
AdV	RW	n = 5	—	—	—	—	—	—	—	—	—	—	—	2	1	5
	Cochleostomy	n = 3	1	—	2	3	—	—	—	—	—	—	1	2	—	3

Abbreviations: AAV, adeno-associated virus; AdV, adenovirus; RW, round window.

^aAAV or AdV was applied to the cochlea via the RW or cochleostomy approach. Transgene expression the various cells of the inner ear was detected by the presence of green fluorescent protein.

^bA dash (—) indicates no fluorescence in cells of the infected mouse cochlea.

FIG. 3. ABR thresholds in mice after gene transfer. Threshold shifts at all frequencies were less than 15 dB in comparison with the contralateral side (*right*, solid circles) after the injection of AAV (**A**) or AdV (**B**) into the scala tympani (*left*, solid squares). On the other hand, injection of AAV (**C**) or AdV (**D**) into the scala media resulted in an elevation of ABR thresholds at all frequencies.



RW approach) and viral vector (AAV) for the neonatal mouse cochlea. The extent of AdV transfection was extremely limited in the mesenchymal cells, comparable to that obtained with adult mice; gene expression after AAV transfection by the RW approach was seen mainly in the cochlear supporting cells.

AAV serotype 1 was chosen on the basis of previously published reports indicating that AAV serotype 2 was unable to transduce hair cells or supporting cells of the cochlea either *in vivo* or *in vitro* (Kho *et al.*, 2000; Jero *et al.*, 2001a; Luebke *et al.*, 2001). There have been no reports demonstrating gene expression in supporting cells without hearing loss after injection into either the neonatal or adult mouse cochlea (Lalwani *et al.*, 1996, 1998; Jero *et al.*, 2001a; Luebke *et al.*, 2001; Duan *et al.*, 2002; Liu *et al.*, 2005, 2007).

When administering AdV in a cochlear organ culture, transgene expression was seen in most hair cells on P0 and in supporting cells on P3 to P5 (Kanzaki *et al.*, 2002). This study also demonstrates that AdV-mediated transgene expression was seen in both hair cells and supporting cells. On the other hand, transduction of P0 explants with AAV serotype 1 thus results in expression in the inner and outer hair cells, Hensen cells, and interdental cells (Stone *et al.*, 2005). In the present study, gene expression was also found mainly in supporting cells and inner hair cells on P0 *in vivo*, but not in supporting cells of the adult mouse as reported in previous studies. The difference in gene expression between adult and neonate may be explained in that supporting cells of the adult mouse do not have sialic acid on their surface as receptors for viral entry whereas those of the neonatal mouse do.

There are a number of genetic diseases that affect the cochlea

early in life. *GJB2*, encoding gap junctional protein connexin26 (Cx26), which is expressed in supporting cells of the organ of Corti, is responsible for approximately half of all hereditary deafness cases (Kelsell *et al.*, 1997; Chang *et al.*, 2003). Animal models of both a conditional knockout of *Gjb2* (Cohen-Salmon *et al.*, 2002) and a dominant-negative *Gjb2* mutation (Kudo *et al.*, 2003) suggest that a critical but unknown function of the supporting cells is disturbed primarily by defective Cx26. Cx26 in the organ of Corti is extensively expressed in the mouse cochlea from birth (Frenz and Water, 2000; Zhang *et al.*, 2005). Furthermore, a dominant-negative *Gjb2* mutant mouse showed incomplete development of the cochlear supporting cells in our preliminary data. Thus, it is possible that the *Gjb2* mutation could be successfully treated by gene delivery to introduce the normal gene to the supporting cells of the neonatal cochlea.

In conclusion, this study has demonstrated excellent gene expression in supporting cells of the neonatal mouse cochlea, with good preservation of auditory function. It is therefore considered to be possible to repair hearing loss by applying the present method to the animal model of the *Gjb2* mutation, thereby suggesting the potential future effectiveness of such a modality for the development of gene-based therapies for humans.

ACKNOWLEDGMENTS

The authors thank Ms. J. Onoda, Mr. T. Yasuda, and Ms. T. Nihira for valuable technical assistance.

AUTHOR DISCLOSURE STATEMENT

No competing financial interests exist.

REFERENCES

- CHANG, E.H., VAN CAMP, G., and SMITH, R.J. (2003). The role of connexins in human disease. *Ear Hear.* **24**, 314–323.
- COHEN-SALMON, M., OTT, T., MICHEL, V., HARDELIN, J.P., PERFETTINI, I., EYBALIN, M., WU, T., MARCUS, D.C., WANGEMANN, P., WILLECKE, K., and PETIT, C. (2002). Target ablation of connexin26 in the inner ear epithelial gap junction network causes hearing impairment and cell death. *Curr. Biol.* **12**, 1106–1111.
- DERBY, M.L., SENA-ESTEVEZ, M., BREAKFIELD, X.O., and COREY, D.P. (1999). Gene transfer into the mammalian inner ear using HSV-1 and vaccine virus vectors. *Hear. Res.* **134**, 1–8.
- DUAN, M.L., BORDET, T., MEZZINA, M., KAHN, A., and ULFENDAHL, M. (2002). Adenoviral and adeno-associated viral vector mediated gene transfer in the guinea pig cochlea. *Neuroreport* **13**, 1295–1299.
- EISEN, M.D., and RYUGO, D.K. (2007). Hearing molecules: Contributions from genetic deafness. *Cell. Mol. Life Sci.* **64**, 566–580.
- FRENZ, C.M., and WATER, T.R. (2000). Immunolocalization of connexin26 in the developing mouse cochlea. *Brain Res. Rev.* **32**, 172–180.
- HAN, J.J., MHATRE, A.N., WAREING, M., PETTIS, R., ZUFFEREY, A.N., TRONO, D., and LALWANI, A.K. (1999). Transgene expression in the guinea pig cochlea mediated by the lentivirus-derived gene transfer vector. *Hum. Gene Ther.* **10**, 1867–1874.
- ISHIMOTO, S., KAWAMOTO, K., KANZAKI, S., and RAPHAEL, Y. (2002). Gene transfer into supporting cells of organ of Corti. *Hear. Res.* **173**, 187–197.
- JERO, J., MHATRE, A.N., TSENG, C.J., STERN, R.E., COLING, D.E., GOLDSTEIN, J.A., HONG, K., ZHENG, W.W., HOQUE, A.T.M.S., and LALWANI, A.K. (2001a). Cochlear gene delivery through an intact round window membrane in mouse. *Hum. Gene Ther.* **12**, 539–548.
- JERO, J., TSENG, C.J., MHATRE, A.N., and LALWANI, A.K. (2001b). A surgical approach appropriate for targeted cochlear gene therapy in the mouse. *Hear. Res.* **151**, 106–114.
- KANZAKI, S., OGAWA, K., CAMPER, S.A., and RAPHAEL, Y. (2002). Transgene expression in neonatal mouse inner ear explants mediated by first and advanced generation adenovirus vectors. *Hear. Res.* **169**, 112–120.
- KANZAKI, S., SHIOTANI, A., INOUE, M., HASEGAWA, M., and OGAWA, K. (2007). Sendai virus vector-mediated transgene expression in the cochlea *in vivo*. *Audiol. Neurotol.* **12**, 119–126.
- KAWAMOTO, K., OH, S.H., KANZAKI, S., BROWN, N., and RAPHAEL, Y. (2001). The function and structural outcome of inner ear gene transfer via the vestibular and cochlear fluids in mice. *Mol. Ther.* **4**, 575–585.
- KELSELL, D.P., DUNLOP, J., STEVENS, H.P., LENCH, N.J., LIANG, J.N., PARRY, G., MUELLER, R.F., and LEIGH, I.M. (1997). Connexin26 mutations in hereditary non-syndromic sensorineural deafness. *Nature* **387**, 80–83.
- KHO, S.T., PETTIS, R.M., MHATRE, A.N., and LALWANI, A.K. (2000). Safety of adeno-associated virus as cochlear gene transfer vector: Analysis of distant spread beyond injected cochleae. *Mol. Ther.* **2**, 368–373.
- KUDO, T., KURE, S., IKEDA, K., XIA, A.P., KATORI, Y., SUZUKI, M., KOJIMA, K., ICHINOHE, A., SUZUKI, Y., AOKI, Y., KOBAYASHI, T., and MATSUBARA, Y. (2003). Transgenic expression of a dominant-negative connexin26 causes degeneration of the organ of Corti and non-syndromic deafness. *Hum. Mol. Genet.* **12**, 995–1004.
- LALWANI, A.K., WALSH, B.J., REILLY, P.G., MUZYCZKA, N., and MHATRE, A.N. (1996). Development of *in vivo* gene therapy for hearing disorders: Introduction of adeno-associated virus into the cochlea of the guinea pig. *Gene Ther.* **3**, 588–592.
- LALWANI, A.K., WALSH, B.J., REILLY, P.G., CARVALHO, G.J., ZOLOTUKHIN, S., MUZYCZKA, N., and MHATRE, A.N. (1998). Long-term *in vivo* cochlear transgene expression mediated by recombinant adeno-associated virus. *Gene Ther.* **5**, 277–281.
- LIU, Y., OKADA, T., SHEYKHOLESAMI, K., SHIMAZAKI, K., NOMOTO, T., MURAMATSU, S.I., KANAZAWA, T., TAKEUCHI, K., AJALLI, R., MIZUKAMI, H., KUME, A., ICHIMURA, K., and OZAWA, K. (2005). Specific and efficient transduction of cochlear inner hair cells with recombinant adeno-associated virus type 3 vector. *Mol. Ther.* **12**, 725–733.
- LIU, Y., OKADA, T., NOMOTO, T., KE X., KUME, A., OZAWA, K., and XIAO, S. (2007). Promoter effects of adeno-associated viral vector for transgene expression in the cochlea *in vivo*. *Exp. Mol. Med.* **39**, 170–175.
- LUEBKE, A.E., FOSTER, P.K., MULLER, C.D., and PEEL, A.L. (2001). Cochlear function and transgene expression in the guinea pig cochlea, using adenovirus- and adeno-associated virus-directed gene transfer. *Hum. Gene Ther.* **12**, 773–781.
- RAPHAEL, Y., FRISANCHO, J.C., and ROESSLER, B.J. (1996). Adenoviral-mediated gene transfer into guinea pig cochlear cells *in vivo*. *Neurosci. Lett.* **207**, 137–141.
- SAMBROOK, J., and RUSSELL, D.W. (2001). Calcium-phosphate-mediated transfection of eukaryotic cells with plasmid DNAs. In: Irwin, N., and Janssen, K.A., eds. *Molecular Cloning: A Laboratory Manual*, 3rd ed. (Cold Spring Harbor Laboratory Press, New York) pp. 16.14–16.20.
- STONE, I.M., LURIE, D.I., KELLEY, M.W., and POULSEN, D.J. (2005). Adeno-associated virus-mediated gene transfer to hair cells and support cells of the murine cochlea. *Mol. Ther.* **11**, 843–848.
- SUZUKI, M., YAMASOBA, T., SUZUKAWA, K., and KAGA, K. (2003). Adenoviral vector gene delivery via the round window membrane in guinea pig. *Neuroreport* **14**, 1951–1955.
- YAMADA, M., IWATSUBO, T., MIZUNO, Y., and MOCHIZUKI, H. (2004). Overexpression of α -synuclein in rat substantia nigra results in loss of dopaminergic neurons, phosphorylation of α -synuclein and activation of caspase-9: Resemblance to pathogenetic changes in Parkinson's disease. *J. Neurochem.* **91**, 451–461.
- ZHANG, Y., TANG, W., AHMED, S., SIPP, J.A., CHEN, P., and LIN, X. (2005). Gap junction-mediated intercellular biochemical coupling in cochlear supporting cells is required for normal cochlear functions. *Proc. Natl. Acad. Sci. U.S.A.* **102**, 15201–15206.

Address reprint requests to:

Dr. Takashi Iizuka
Department of Otorhinolaryngology
Juntendo University School of Medicine
2-1-1 Hongo, Bunkyo-ku
Tokyo 113-8421, Japan

E-mail: t-iizuka@med.juntendo.ac.jp

Received for publication December 6, 2007; accepted after revision February 19, 2008.

Published online: March 26, 2008.

Neurobiology

Mesenchymal Stem Cell Transplantation Accelerates Hearing Recovery through the Repair of Injured Cochlear Fibrocytes

Kazusaku Kamiya,* Yoshiaki Fujinami,*
Noriyuki Hoya,* Yasuhide Okamoto,*
Hiroko Kouike,* Rie Komatsuzaki,*
Ritsuko Kusano,* Susumu Nakagawa,*
Hiroko Satoh,† Masato Fujii,‡ and
Tatsuo Matsunaga*

From the Laboratory of Auditory Disorders* and Division of Hearing and Balance Research,† National Institute of Sensory Organs, and the Department of Plastic Surgery,‡ National Tokyo Medical Center, Tokyo, Japan

Cochlear fibrocytes play important roles in normal hearing as well as in several types of sensorineural hearing loss attributable to inner ear homeostasis disorders. Recently, we developed a novel rat model of acute sensorineural hearing loss attributable to fibrocyte dysfunction induced by a mitochondrial toxin. In this model, we demonstrate active regeneration of the cochlear fibrocytes after severe focal apoptosis without any changes in the organ of Corti. To rescue the residual hearing loss, we transplanted mesenchymal stem cells into the lateral semicircular canal; a number of these stem cells were then detected in the injured area in the lateral wall. Rats with transplanted mesenchymal stem cells in the lateral wall demonstrated a significantly higher hearing recovery ratio than controls. The mesenchymal stem cells in the lateral wall also showed connexin 26 and connexin 30 immunostaining reminiscent of gap junctions between neighboring cells. These results indicate that reorganization of the cochlear fibrocytes leads to hearing recovery after acute sensorineural hearing loss in this model and suggest that mesenchymal stem cell transplantation into the inner ear may be a promising therapy for patients with sensorineural hearing loss attributable to degeneration of cochlear fibrocytes. (*Am J Pathol* 2007, 171:214–226; DOI: 10.2353/ajpath.2007.060948)

Mammalian cochlear fibrocytes of the mesenchymal non-sensory regions play important roles in the cochlear

physiology of hearing, including the transport of potassium ions to generate an endocochlear potential in the endolymph that is essential for the transduction of sound by hair cells.^{1–3} It has been postulated that a potassium recycling pathway toward the stria vascularis via fibrocytes in the cochlear lateral wall is critical for proper hearing, although the exact mechanism has not been definitively determined.² One candidate model for this ion transport system consists of an extracellular flow of potassium ions through the scala tympani and scala vestibuli and a transcellular flow through the organ of Corti, supporting cells, and cells of the lateral wall.^{4,5} The fibrocytes within the cochlear lateral wall are divided into type I to V based on their structural features, immunostaining patterns, and general location.⁵ Type II, type IV, and type V fibrocytes resorb potassium ions from the surrounding perilymph and from outer sulcus cells via the Na,K-ATPase. The potassium ions are then transported to type I fibrocytes, stria basal cells, and intermediate cells through gap junctions and are secreted into the intrastrial space through potassium channels. The secreted potassium ions are incorporated into marginal cells by the Na,K-ATPase and the Na-K-Cl co-transporter, and are finally secreted into the endolymph through potassium channels.

Degeneration and alteration of the cochlear fibrocytes have been reported to cause hearing loss without any other changes in the cochlea in the Pit-Oct-Unc (POU)-domain transcription factor Brain-4 (Brn-4)-deficient mouse⁶ and the otospiralin-deficient mouse.³ Brn-4 is the gene responsible for human DFNB3, an X chromosome-linked nonsyndromic hearing loss. Mice deficient in Brn-4 exhibit reduced endocochlear potential and hearing loss and show severe ultrastructural alterations, including cel-

Supported by the Ministry of Health, Labor, and Welfare of Japan (health science research grant H16-kankakuki-006 to T.M.) and the Japan Foundation for Aging and Health (to K.K.).

Accepted for publication March 26, 2007.

Address reprint requests to Dr. Tatsuo Matsunaga, Laboratory of Auditory Disorders, National Institute of Sensory Organs (NISO), National Tokyo Medical Center, 2-5-1 Higashigaoka, Meguro-ku, Tokyo 152-8902, Japan. E-mail: matsunagatatsuo@kankakuki.go.jp.

lular atrophy and a reduction in the number of mitochondria, exclusively in spiral ligament fibrocytes.^{6,7} In the otospiralin-deficient mouse, degeneration of type II and IV fibrocytes is the main pathological change, and hair cells and the stria vascularis appear normal.³ Furthermore, in mouse and gerbil models of age-related hearing loss,⁸⁻¹⁰ degeneration of the cochlear fibrocytes precede the degeneration of other types of cells within the cochlea, with notable pathological changes seen especially in type II, IV, and V fibrocytes. In humans, mutations in the connexin 26 (*Cx26*) and connexin 30 (*Cx30*) genes, which encode gap junction proteins and are expressed in cochlear fibrocytes and nonsensory epithelial cells, are well known to be responsible for hereditary sensorineural deafness.^{11,12} These instances of deafness related to genetic, structural, and functional alterations in the cochlear fibrocytes highlight the functional importance of these fibrocytes in maintaining normal hearing.

Recently, we developed an animal model of acute sensorineural hearing loss attributable to acute cochlear energy failure by administering the mitochondrial toxin 3-nitropropionic acid (3NP) into the rat round window niche.^{13,14} 3NP is an irreversible inhibitor of succinate dehydrogenase, a complex II enzyme of the mitochondrial electron transport chain.^{15,16} Systemic administration of 3NP has been used to produce selective striatal degeneration in the brain of several mammals.^{17,18} Our model with 3NP administration into the rat cochlea showed acute sensorineural hearing loss and revealed an initial pathological change in the fibrocytes of the lateral wall and spiral limbus without any significant damage to the organ of Corti or spiral ganglion. Furthermore, depending on the dose of 3NP used, these hearing loss model rats exhibited either a permanent threshold shift or a temporary threshold shift. In the present study, we used doses of 3NP that induce temporary threshold shift to explore the mechanism of hearing recovery after injury to the cochlear fibrocytes and examined a novel therapeutic approach to repair the injured area using mesenchymal stem cell (MSC) transplantation.

MSCs are multipotent cells that can be isolated from adult bone marrow and can be induced to differentiate into a variety of tissues *in vitro* and *in vivo*.¹⁹ Human MSCs transplanted into fetal sheep intraperitoneally undergo site-specific differentiation into chondrocytes, adipocytes, myocytes, cardiomyocytes, bone marrow stromal cells, and thymic stroma.²⁰ Furthermore, when MSCs were transplanted into postnatal animals, they could engraft and differentiate into several tissue-specific cell types in response to environmental cues provided by different organs.²¹ These transplantability features of MSCs suggested the possibility that they could restore hearing loss in 3NP-treated rats to the normal range. Recently, experimental bone marrow transplantation into irradiated mice suggested that a part of spiral ligament that consists of cochlear fibrocytes was derived from bone marrow cells or hematopoietic stem cells.²² This indicates that bone marrow-derived stem cells such as MSCs may have a capacity to repair the injury of cochlear fibrocytes. In this study, we demonstrate that MSC transplantation significantly improves hearing recovery, and

present evidence suggesting invasion of transplanted MSCs into the injured region of the cochlear lateral wall and repair of the interrupted gap junction network.

Materials and Methods

Rat Model of Acute Sensorineural Hearing Loss Attributable to Cochlear Fibrocyte-Specific Injury

Experimental procedures reported in this study were approved by the Institutional Animal Care and Use Committee of the National Tokyo Medical Center. Sprague-Dawley rats (Clea Japan, Tokyo, Japan) weighing between 180 and 210 g (8 to 10 weeks old) were used. Before surgery, the animals were anesthetized with pentobarbital (30 to 40 mg/kg, i.p.; Dainippon Pharmaceutical, Osaka, Japan), and after local administration of 1% lidocaine (AstraZeneca PLC, London, UK), an incision was made posterior to the left pinna near the external meatus. The left otic bulla was opened to approach the round window niche. The distal end of a section of PE 10 tubing (Becton-Dickinson, Franklin Lakes, NJ) was drawn to a fine tip in a flame and gently inserted into the round window niche. 3NP (Sigma, St. Louis, MO) was dissolved in saline at 300 mmol/L and the pH adjusted to 7.4 with NaOH. Saline alone was used as a control. The solution was administered for 2 minutes at a rate of 1.5 μ l/minute with a syringe pump. After treatment, a small piece of gelatin was placed on the niche to keep the solution in the niche regardless of head movement, and the wound was closed. The right cochlea was surgically destroyed to avoid cross-hearing during auditory brainstem response (ABR) recording.

Auditory Brainstem Response

ABR recording was performed as previously described¹³ before surgery and at 2 hours and 1, 2, 3, 7, 14, 21, 28, 35, and 42 days after surgery (or until 14 days in the MSC transplantation experiment). Six to 12 rats in each group were used for the recordings. ABR was recorded using Scope waveform storing and stimulus control software and the PowerLab data acquisition and analysis system (PowerLab2/20; AD Instruments, Castle Hill, Australia). Electroencephalogram recording was performed using a digital Bioamp extracellular amplifier system (BAL-1; Tucker-Davis Technologies, Alachua, FL). Sound stimuli were produced by a coupler type speaker (ES1spc; Bio Research Center, Nagoya, Japan) inserted into the ear canal. Pure tone bursts of 8, 20, and 40 kHz (0.2-ms rise/fall time and 1-ms flat segment) were generated, and the amplitude was specified by a real-time processor and programmable attenuator (RP2.1 and PA5; Tucker-Davis Technologies). Sound level calibration and frequency confirmation were performed using a 1/4 inch free-field mic (7016; ACO Pacific, Belmont, CA), microphone amp (MA3; Tucker-Davis Technologies), a digital oscilloscope (DS-8822P; Iwatsu Electronic, Tokyo, Japan), and a sound level meter (NL32; Rion, Tokyo, Japan). The maximum output level was 87, 86, and 96 dB at 8, 20, and 40

kHz, respectively. For recording, the animals were anesthetized with pentobarbital before stainless steel needle electrodes were placed ventrolateral to the ears. Waveforms of 512 stimuli at a frequency of 9 Hz were averaged, and the visual detection threshold was determined by increasing or decreasing the sound pressure level in 5-dB steps. The effects of 3NP and/or MSC transplantation on the ABR threshold and recovery ratio of ABR threshold (peak threshold – threshold at 14 days or 42 days/peak threshold \times 100) were statistically analyzed at each frequency using an unpaired Student's *t*-test. The significance level for all statistical procedures was set at $P < 0.05$.

Bromodeoxyuridine (BrdU) Injection

To detect cell proliferation in the rat inner ear, BrdU (Sigma) was injected (30 mg/kg i.p. per single injection) as previously described.²³ Injections were started just after 3NP administration and continued every 12 hours for 3 or 6 days.

MSC Preparation

We previously established bone marrow MSCs and demonstrate their potential to differentiate into several cell types.²⁴ The cells were prepared from 6- to 8-week-old male F344 rats (Clea) as described. In brief, surgical treatment was performed after intraperitoneal injection of pentobarbital (30 to 40 mg/kg, i.p.). After surgery, the rats were sacrificed by ether inhalation followed by dislocation of the neck. Rat femurs and tibiae were collected and the long bones meticulously dissected to remove all adherent soft tissue. Both ends of the bones were cut away from the diaphyses with bone scissors. The bone marrow plugs were hydrostatically expelled from the bones by inserting 18-gauge needles fastened to 10-ml syringes filled with complete medium [Dulbecco's modified Eagle's medium (Sigma), 10% fetal bovine serum (Sigma), and 100 U/ml penicillin-streptomycin (Sigma)] into the distal ends of the femora and the proximal ends of the tibiae. Cells were plated on plastic culture dishes. The nonadherent cell population was removed after 24 hours, and the adherent layer was washed once with fresh media. The cells were then continuously cultured for 1 to 4 weeks in complete medium. Medium was completely replaced every 3 days. When the cells were nearly confluent, the adherent cells were released from the dishes with 0.25% trypsin-ethylenediaminetetraacetic acid (Sigma), split 1:3, and seeded onto fresh plates. Cells from passages 10 to 15 were stored with Cell Banker reagent (Juji Field, Tokyo, Japan) in liquid nitrogen. The frozen cell suspensions were thawed at 1 week before the transplantation and cultured in complete medium at 37°C in a humidified atmosphere of 5% CO₂. The potential of these cells as MSCs were previously demonstrated as described.²⁴ The surface marker expression of these cells was analyzed by flow cytometry (Epics Altra with HyPerSort cell sorting system; Beckman Coulter, Fullerton, CA). At ~80 to 90% confluence, MSCs were disso-

ciated by treatment with 1 \times Accutase (Chemicon International, Temecula, CA) for 15 minutes at 37°C followed by phosphate-buffered saline (PBS) washout, centrifugation at 1200 rpm for 10 minutes, and resuspension in Hanks' balanced salt solution (HBSS)⁺ medium [HBSS⁻ medium (Invitrogen Japan, Tokyo, Japan) with 2% fetal bovine serum and 10 mmol/L 2-[4-(2-hydroxyethyl)-1-piperazinyl]ethanesulfonic acid (HEPES) buffer (Invitrogen Japan)]. MSCs were incubated with antibodies against CD45, CD31, CD29, CD44H, CD54, CD73, and CD90 (BD PharMingen, San Diego, CA) for 30 minutes on ice and spun down. At the end of the staining, MSCs were resuspended in ice-cold HBSS⁺ medium containing 2 μ g/ml propidium iodide for discrimination of dead cells. To detect the MSCs after injection, cultured MSCs were incubated with 5 μ mol/L BrdU for 2 days before transplantation as previously described.²⁵

MSC Transplantation

Before transplantation, cultured MSCs were released from the dishes with 0.25% trypsin-ethylenediaminetetraacetic acid and washed by centrifugation with Dulbecco's phosphate-buffered saline (D-PBS; Invitrogen Japan) and resuspended to prepare MSC suspension (1 \times 10⁵ cells in 20 μ l of D-PBS) for the following transplantation. Three days after 3NP administration, the rats were anesthetized with pentobarbital (30 to 40 mg/kg, i.p.) and by local administration of 1% lidocaine. Incisions were made as described for 3NP administration, the surfaces of the posterior and lateral semicircular canals were exposed, and a small hole was made in each canal. A small tube (Eicom, Kyoto, Japan) was inserted into the lateral semicircular canal toward the ampulla. Through this tube, the perilymph was perfused with an MSC suspension (1 \times 10⁵ cells in 20 μ l of D-PBS) for 10 minutes at a rate of 2 μ l/minute using a syringe pump with drainage from the hole made on the posterior semicircular canal. The tube was then removed, the holes on the semicircular canals were sealed with a muscle and fibrin adhesive (Beriplast P Combi-set; CSL Behring, King of Prussia, PA), and the wound on the neck was closed. An equal volume of vehicle (D-PBS) was also injected into the semicircular canal of 3NP-treated rats as control.

Tissue Preparation

The rats were sacrificed at 3 days (three rats for 3NP and three rats for saline control) and 42 days (five rats for 3NP and three rats for saline control) after 3NP treatment and 11 days after MSC transplantation (12 rats for 3NP with MSC transplantation, seven rats for MSC transplantation only, and five rats for 3NP followed by vehicle injection). They were deeply anesthetized with pentobarbital and transcardially perfused with 0.01 mol/L phosphate buffer, pH 7.4, containing 8.6% sucrose followed by a fixative consisting of freshly depolymerized 4% paraformaldehyde in 0.1 mol/L phosphate buffer (pH 7.4). After decapitation, the left temporal bones were removed and immediately placed in the same fixative. Small openings

were made at the round window, oval window, and the apex of the cochlea. After overnight immersion in fixative, the temporal bones were decalcified by immersion in 5% sucrose, 5% ethylenediaminetetraacetic acid, pH 7.4, with stirring at 4°C for 14 days. The specimens were dehydrated through graded concentrations of alcohol, embedded in paraffin blocks, and sectioned into 5- μ m-thick slices. The sections were stained with hematoxylin and eosin (H&E) as generally described, by terminal deoxynucleotidyl transferase (TdT)-mediated dUTP nick-end labeling (TUNEL) and by immunohistochemistry for BrdU, Cx30, or Cx26 as described below.

TUNEL Assay

TUNEL assays were performed using an ApopTag Fluorescein Direct *in situ* apoptosis detection kit (Chemicon International) according to the manufacturer's instructions. In brief, specimens were digested with 20 μ g/ml proteinase K in 0.01 mol/L PBS, pH 7.4, for 5 minutes, incubated with TdT and fluorescein-labeled nucleotide in a humid atmosphere at 37°C for 1 hour, and then incubated with 2 μ mol/L TOPRO-3 iodide (Molecular Probes, Eugene, OR) for 5 minutes. The specimens were viewed with a confocal laser microscope (LSM510; Carl Zeiss, Esslingen, Germany; or Radiance 2100; Bio-Rad, Hercules, CA), and each image was analyzed and saved by ZeissLSM image browser (Carl Zeiss). Negative controls included proteinase K digestion but did not include TdT so that nonspecific incorporation of nucleotide, or nonspecific binding of enzyme-conjugate, could be assessed. Distilled water was substituted for TdT enzyme reagent in negative controls.

Immunohistochemistry

After pretreatment with 2 mol/L HCl at 37°C for 30 minutes, incubation with 20 μ g/ml proteinase K in PBS for 5 minutes, and incubation with blocking solution (1.5% normal goat serum in PBS) for 30 minutes at room temperature, tissue sections were incubated with anti-BrdU antibody (DAKO, Glostrup, Denmark) diluted 1:100 in PBS for 30 minutes, then with biotin-conjugated anti-mouse IgG (Vector, Burlingame, CA) diluted 1:200 in PBS for 30 minutes, followed by horseradish peroxidase (HRP)-conjugated streptavidin-biotin complex (streptABCComplex-HRP, Vectastain Elite ABC kit standard; Vector) for 1 hour at room temperature. Sections were stained in DAB-H₂O₂ (Vector) for 3 minutes and hematoxylin for 1 minute and then rinsed and covered with a coverslip. For BrdU and TUNEL double staining, Alexa568-conjugated anti-mouse IgG (1:600; Molecular Probes) was used as a secondary antibody in the BrdU staining after the TUNEL procedure. For double-staining of BrdU with Cx30 or Cx26, rabbit anti-Cx26 (1:300; Zymed Laboratories, South San Francisco, CA) or rabbit anti-Cx30 (1:400; Zymed Laboratories) antibody and anti-BrdU antibody were used as a primary antibody cocktail, and Alexa488-conjugated anti-rabbit IgG (1:400; Molecular Probes) with Alexa568-conjugated anti-mouse IgG were used as

a secondary antibody cocktail. For nuclear staining, TO-PRO-3 iodide (2 μ mol/L; Molecular Probes), 4,6-diamidino-2-phenylindole (1 μ g/ml; Dojindo Laboratories, Kumamoto, Japan) or propidium iodide (1 μ g/ml; Molecular Probes) was used. Negative controls were performed without primary antibodies to assess nonspecific binding of the secondary antibody or of the streptABCComplex-HRP. Inner ear sections that were not injected with BrdU were also used as negative controls. Background autofluorescence was not observed in the cochlear sections with the tissue preparation methods used in the present study.

Results

Long-Term Observation of Temporary Threshold Shift and Hearing Recovery after 3NP Administration

We monitored ABR thresholds in 3NP-treated rats at 8, 20, and 40 kHz for 42 days after 3NP administration (Figure 1, A–C) to examine the potential for hearing recovery. At all frequencies, the ABR thresholds peaked 1 day after 3NP administration and then gradually recovered. At 8 kHz ($n = 7$), the threshold reached within a normal threshold level (11 dB) 42 days after 3NP administration. However, the ABR threshold at 40 kHz showed only a mild recovery after 14 days. The hearing recovery ratio, which is described in Materials and Methods, was calculated for each tested frequency (Figure 1D). At 14 days, the recovery ratios were $73.4 \pm 5.5\%$ for 8 kHz ($n = 11$), $57.0 \pm 11.2\%$ for 20 kHz ($n = 11$), and $37.5 \pm 7.7\%$ for 40 kHz ($n = 12$). At 42 days, they were $97.2 \pm 9.4\%$ for 8 kHz ($n = 7$), $67.0 \pm 16.4\%$ for 20 kHz ($n = 7$), and $32.3 \pm 7.7\%$ for 40 kHz ($n = 7$). Throughout the recovery time course, the recovery ratios at the lower frequencies always tended to be higher than those at the highest frequency. At 42 days, the recovery ratio for 8 kHz was significantly higher than that for 40 kHz ($P = 0.005$). Between 14 and 42 days after 3NP administration, the hearing level for 40 kHz did not show significant recovery, but the recovery ratios for 8 and 20 kHz showed 24 and 10% increases, respectively.

Apoptosis and Regeneration of the Cochlear Fibrocytes after 3NP Administration

To analyze the pathological changes associated with the acute hearing loss observed in the 3NP-treated rats, we performed H&E staining and TUNEL reaction to detect apoptosis. No histological changes were observed in the organ of Corti and spiral ganglion of rats with 3NP administration as shown in Figure 2, A and B. However, severe apoptosis, with chromatin condensation and apoptotic bodies, was observed only in the lateral wall and the spiral limbus at 3 days after 3NP administration (Figure 2, C and D). These severe apoptotic regions included more than 30% TUNEL-positive or apoptotic cells and were clearly demarcated as shown in Figure 2,

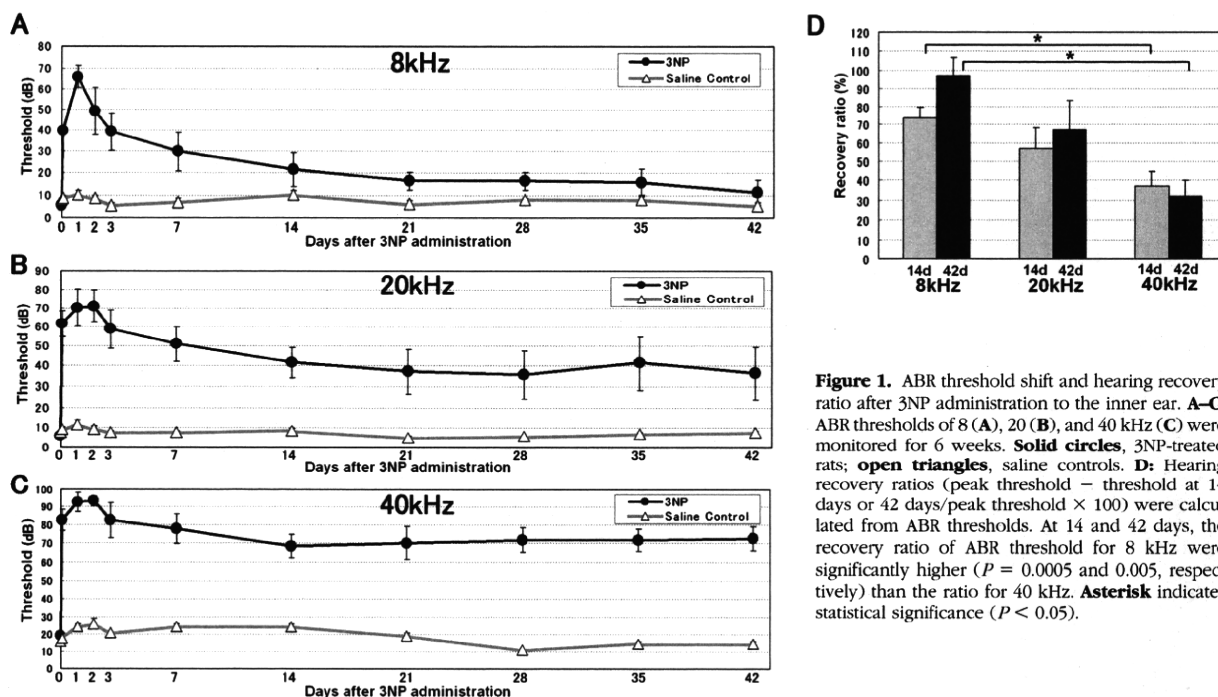


Figure 1. ABR threshold shift and hearing recovery ratio after 3NP administration to the inner ear. **A–C:** ABR thresholds of 8 (**A**), 20 (**B**), and 40 kHz (**C**) were monitored for 6 weeks. **Solid circles**, 3NP-treated rats; **open triangles**, saline controls. **D:** Hearing recovery ratios (peak threshold – threshold at 14 days or 42 days/peak threshold × 100) were calculated from ABR thresholds. At 14 and 42 days, the recovery ratio of ABR threshold for 8 kHz were significantly higher ($P = 0.0005$ and 0.005 , respectively) than the ratio for 40 kHz. **Asterisk** indicates statistical significance ($P < 0.05$).

E and F. These areas contain cochlear fibrocytes that participate in the potassium recycling route within the cochlea. The typical distribution pattern of TUNEL-positive cells after 3NP treatment is shown in Figure 2E, but a few rats with more severe hearing impairment (with ~55 dB elevation of the ABR threshold) demonstrated more prominent histological changes, with focal cell loss in the center surrounded by TUNEL-positive cells (Figure 2, G and H). On light microscopic observation of H&E-stained sections, histological changes suggesting inflammation were not evident in the lateral wall and spiral limbus. As for cochlear turns, lateral wall in basal turn had more severe damage than the middle turn as shown in Figure 4, G, I, and J, and the apical turn had little damage in the lateral wall.

To analyze the mechanism of hearing recovery after damage to the cochlear lateral wall, we performed a BrdU incorporation assay in addition to the TUNEL assay (Figure 3). BrdU-positive cells were observed mainly in the lateral wall fibrocytes and occasionally observed in spiral limbus, Schwann cells, and Reissner's membrane. At 3 days after 3NP administration, the BrdU-positive cell count around the area of apoptosis in the lateral wall was 6.2 ± 0.7 cells (19 cross sections from three rats) compared with 0.5 ± 0.1 cells (12 cross sections from three rats) for the control (Figure 3, A–C). Furthermore, a few TUNEL-positive dying cells that take up BrdU were detected, indicating that some fibrocytes that regenerated after 3NP administration also became apoptotic 3 days after 3NP administration (Figure 3C, arrow). To trace the cells regenerated after the early injury, the rats were continuously injected with BrdU during the first 6 days after 3NP administration and sacrificed 42 days after 3NP administration for detection of BrdU-positive cells. Few TUNEL-positive cells were detected, but a number of

BrdU-positive cells could be detected in the central part of the lateral wall in the middle turn of the cochlea (Figure 3, D–F). At 42 days after 3NP administration, 2.6 ± 0.8 BrdU-positive cells were detected in a cross section of the lateral wall of the middle turn in 3NP-treated rats (26 cross sections from five rats) compared with 0.2 ± 0.2 cells in saline-treated controls (12 cross sections from three rats). In contrast, only a few BrdU-positive cells were detected in the spiral limbus at 3 and 42 days after 3NP administration.

Characterization of MSCs

For the MSC transplantation into inner ear, we used rat bone marrow-derived cells, which we previously established and demonstrated their capacity for differentiation as MSC.²⁴ Flow cytometry of these MSCs before the transplantation demonstrated surface expression of CD29, CD44H, CD54, CD73, and CD90, but not of CD31 or CD45. This surface expression pattern was similar to human and murine MSCs.^{26,27}

Transplantation and Detection of MSCs in the Inner Ear Tissue

To improve the hearing recovery of high-frequency (40 kHz) sounds, we transplanted BrdU-labeled MSCs into the inner ear of 3NP-treated rats using perilymphatic perfusion with MSC suspension from the lateral semicircular canal. Eleven days after transplantation, a number of BrdU-positive cells were observed along the ampullary crest surface facing the perilymph in the lateral semicircular canal that was closest to the site of MSC injection (Figure 4A, arrow), suggesting that the transplanted